A practical method for determining film thickness using X-ray absorption spectroscopy in total electron yield mode

Noritake Isomura,* Keiichiro Oh-ishi, Naoko Takahashi and Satoru Kosaka

Toyota Central R&D Laboratories Inc., 41-1 Yokomichi, Nagakute, Aichi 480-1192, Japan.
*Correspondence e-mail: isomura@mosk.tytlabs.co.jp

Thin films formed on surfaces have a large impact on the properties of materials and devices. In this study, a method is proposed using X-ray absorption spectroscopy to derive the film thickness of a thin film formed on a substrate using the spectral separation and logarithmic equation, which is a modified version of the formula used in electron spectroscopy. In the equation, the decay length in X-ray absorption spectroscopy is longer than in electron spectroscopy due to a cascade of inelastic scattering of electrons generated in a solid. The modification factor, representing a multiple of the decay length, was experimentally determined using oxidized Si and Cu with films of thickness 19 nm and 39 nm, respectively. The validity of the proposed method was verified, and the results indicated that the method can be used in the analysis of various materials with thin films.

1. Introduction

Thin films formed on a surface have a great impact on the properties of materials and devices (Kaiser, 2002). In the case of optical films, such as anti-reflective films, and functional films, such as hydrophilic films, the designed film itself often characterizes the product (Hata *et al.*, 2000). In addition, there are cases where a film is formed during use. For example, in lithium-ion batteries (LIBs), a film is formed on the surface of the negative electrode by the decomposition of the electrolyte (Cheng *et al.*, 2016). The thickness of the film is one of the main factors determining battery performance; namely, a thin film increases the decomposition reaction of the electrolyte, while a thick film increases the electrical resistance (Kawaura *et al.*, 2016).

In optical and functional films, substrates with smooth surfaces are typically used, making it easy to measure and control the film thickness. However, as in the case of LIBs, there are various materials with particles or uneven surfaces, making it difficult to measure the film thickness. Although the film thickness can be measured by cross-sectional observation using an electron microscope (Truijen *et al.*, 2007; Ishida & Sato, 2003), the thickness may be local and specific to a particular location. Although local information is important, the average film thickness is often necessary to understand the characteristics of the material. Hard X-ray photoelectron spectroscopy can provide the average film thickness by data analysis, but the analysis depth is shallow, around 10 nm (Powell & Tanuma, 2016). This means that this is insufficient, for example, to measure the film of LIBs.

X-ray absorption spectroscopy (XAS) provides information about the chemical states of the target element (Norman,
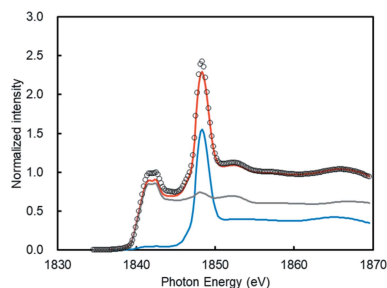
1986). XAS measurements in the total electron yield (TEY) mode, referred to as TEY-XAS, have an analysis depth of several tens of nanometres, especially when using hard X-rays (Schroeder *et al.*, 1995), where the electron signal intensity becomes 1/e due to the attenuation caused by a cascade of inelastic scattering of electrons generated in a solid (Girardeau *et al.*, 1992; Abbate *et al.*, 1992). TEY-XAS measurements are applied to the analysis of films with thicknesses in the range of several tens of nanometres. Although the XAS spectra can be separated into film and substrate components by linear combination fitting (LCF) using standard spectra (Isomura *et al.*, 2017), calculation of film thickness has not been performed in TEY-XAS. However, the calculation is performed in the field of electron spectroscopy, and the film thickness d is given by the following equation (Strohmeier, 1990),

$$d = \lambda_f \sin \theta \ln \left[\frac{N_s \lambda_s}{N_f \lambda_f} \frac{I_f}{I_s} + 1 \right], \qquad (1)$$

where λ is the inelastic mean free path of electrons (Tanuma *et al.*, 1994), corresponding to the depth of analysis at which the intensity decays to 1/e. θ is the detection angle, N is the atomic density, I is the detection intensity, and subscripts f and s refer to the film and substrate, respectively. Equation (1) is based on the theory of inelastic scattering of electrons and represents the exponential decay of the substrate component with respect to the film thickness. This theory and decay are common to TEY-XAS (Abbate *et al.*, 1992); thus, it is possible that equation (1) may also be used to calculate the film thickness in TEY-XAS, but with a different value of λ (specifically, k times) because the cascade of inelastic scattering specific to TEY-XAS increases the decay length (Abbate *et al.*, 1992).

The analysis depth (sometimes referred to as probing depth in the literature) in TEY has been investigated in the low-energy region using soft X-rays (Frazer *et al.*, 2003; Abbate *et al.*, 1992; Kasrai *et al.*, 1996; Ruosi *et al.*, 2014), and in TEY and conversion electron yield (CEY) in the high-energy region using hard X-rays (Girardeau *et al.*, 1992; Bouldin *et al.*, 1987; Elam *et al.*, 1988; Erbil *et al.*, 1988; Schroeder, 1997). In these reports, Elam *et al.* (1988) proposed an equation using Huffman's equation with a correction factor applied. However, only Fe was studied, and the factor was corrected to fit this case.

In this study, we propose a practical method to derive the film thickness for TEY-XAS by modifying equation (1). The factor k was obtained experimentally using oxidized Si and Cu with films of known thicknesses, which have relatively small and large atomic numbers, respectively.

2. Methodology

The specific procedure for deriving the film thickness is described below.

(i) The X-ray absorption near-edge structure (XANES) spectrum is obtained by TEY-XAS measurement.

(ii) The obtained spectrum is separated into film and substrate components by LCF using standard spectra of the film and substrate.

(iii) The film thickness d is calculated by substituting each value into equation (2), which is a modified version of equation (1) for TEY-XAS,

$$d = k\lambda_f \ln \left[\frac{N_s \lambda_s}{N_f \lambda_f} \frac{I_f}{I_s} + 1 \right], \qquad (2)$$

where k is a factor determined experimentally in this study, and λ is obtained using the *QUASES-IMFP-TPP2M* software (Tougaard, 2000), which is based on the model proposed by Tanuma *et al.* (1994). k is assumed to be the same regardless of the film and substrate, because the dependence on the material is reflected in λ. It should be noted that many electrons emitted from the surface (energy-loss electrons) lose the angular information at the time of generation, and the emission angle is assumed to be approximately 90° on average, resulting in $\sin \theta$ in equation (1) being equal to 1.

3. Experimental

The samples were a Si(100) wafer and Cu plate (99.96% purity) with thin oxide films (hereafter referred to as oxidized Si and oxidized Cu, respectively). The Si oxide film was formed by annealing at 900°C in dry O_2 ambient, and the thickness was 19 nm, which was measured by an ellipsometer (L115C, Gaertner Scientific Co.) with an accuracy of ±3 nm. The Cu oxide film was formed by annealing at 230°C for 10 min in air atmosphere under conditions similar to those used by Valladares *et al.* (2012). The thickness was 39 nm, which was confirmed by cross-sectional transmission electron microscopy (JEM-2100F, Jeol Ltd).

For the oxidized Si, XAS measurement was conducted at the BL6N1 beamline of the Aichi Synchrotron Radiation Center in Japan, which has an electron storage ring with a circumference of 72 m and is operated at an electron energy of 1.2 GeV with a current of 300 mA (Yamamoto *et al.*, 2014). White light from a bending magnet was monochromated by an InSb(111) double-crystal monochromator. The beam size at the sample position was 2 mm (horizontal) × 1 mm (vertical), and the incident angle was 90° relative to the sample surface. The intensity of the XAS measurement was measured by the sample drain current, where the sample was placed in a vacuum chamber (approximately 5×10^{-8} Pa).

For the oxidized Cu, XAS measurements were conducted at the BL16XU and BL16B2 beamlines in the synchrotron radiation facility SPring-8 in Japan, which has an electron storage ring with a circumference of 1436 m and is operated at an electron energy of 8 GeV with a current of 100 mA (Hirai *et al.*, 2004). At BL16XU, quasi-monochromatic light from an undulator was monochromated with a Si(111) double-crystal monochromator. The beam size at the sample position was 0.3 mm (horizontal) × 0.05 mm (vertical). At BL16B2, white light from a bending magnet was monochromated with a Si(111) double-crystal monochromator. The beam size at the sample position was 2 mm (horizontal) × 1 mm (vertical). The

incident angle was 15° relative to the sample surface at both BL16XU and BL16B2. The intensity of the XAS measurement was measured by CEY as well as TEY (Takahashi *et al.*, 1999; Nonaka *et al.*, 2007), generally used for hard X-rays. In TEY-XAS, the sample was placed in vacuum. In CEY-XAS, the sample was placed in He ambient. The distance between the electrode and sample was 10 mm, and the voltage applied to the electrode was 1000 V. The XAS data were analyzed using the data processing software *ATHENA* (Ravel & Newville, 2005).

4. Results and discussion

XANES spectra of the oxidized Si and oxidized Cu are presented in Fig. 1. For the oxidized Si, the peaks at 1842 eV and 1848 eV were assigned to Si and SiO_2, respectively (Owens *et al.*, 2002). For the oxidized Cu, the rising edge of the spectrum (absorption edge) was observed at 8978 eV and was assigned to Cu (metal) (Klysubun *et al.*, 2017). However, the spectral shape was similar but not identical to that of Cu (metal), although there is a slight difference between TEY and CEY. The peak at 8995 eV is characterized by its high intensity, suggesting that Cu_2O was also included (Klysubun *et al.*, 2017). For both the oxidized Si and Cu, the detection of Si and Cu (metal), respectively, indicates that the substrates beneath the oxide films were detected.

The XANES spectra illustrated in Fig. 1 were analyzed by LCF using the standard spectra of the film and substrate, as illustrated in Fig. 2, and the component fractions are presented in Table 1. The fitting errors were small (less than 0.005 for both samples). Table 1 also presents the factor k calculated for the film thickness d calculated by equation (2) to match the sample film thickness, where the parameters of equation (2) were set as follows: $d = 19$, $N_s/N_f = 2.33/2.65$, $\lambda_s/\lambda_f = 3.466/4.204$ for Si; and $d = 39$, $N_s/N_f = 3.16/2.20$, $\lambda_s/\lambda_f = 7.204/8.870$ for Cu. The derived factor k was 6.5 for Si and 6.7 for Cu, with an average value of 6.6. This agreement for the different elements supports the fact that the decay length in TEY-XAS is based on the inelastic scattering of electrons.

The validity of the proposed method was verified. Girardeau *et al.* (1992) investigated the variation of the Cu intensity with film thickness for Cu films (up to 160 nm) formed on SiO_2. The value of the Cu film component was taken from the literature and substituted into equation (2), which was proposed in this study, to obtain the film thickness (Table 2). The results were in relatively good agreement, although the estimate was approximately 20% smaller for thinner films (*e.g.* −1 nm for a film thickness of 5 nm). This agreement supports the validity of the TEY-XAS film thickness derivation method employing equation (2) with a factor k of 6.6.

The reason for the smaller estimate for thinner films may be that the effect of elastic scattering was not included. Some electrons generated in a solid are ejected from the sample without any energy loss due to elastic scattering (Yoshikawa & Shimizu, 1992). As the fraction of these electrons increases, the decay length increases. This influence is relatively large when the film thickness is small. In this method, which does
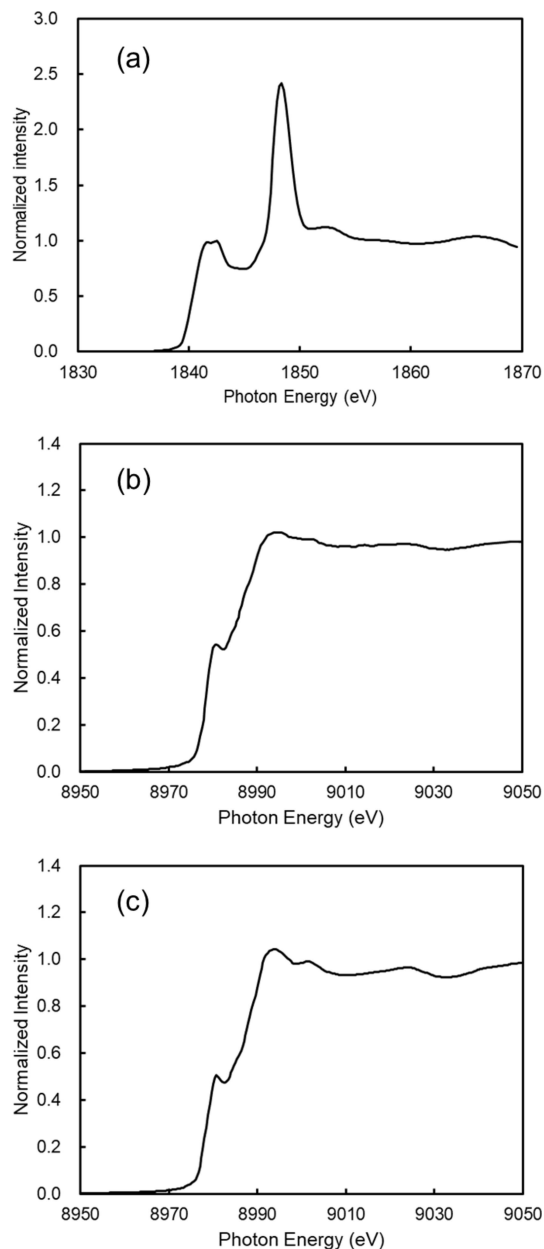
Figure 1
Si *K*-edge and Cu *K*-edge X-ray absorption near-edge structure spectra for oxidized Si (*a*) and oxidized Cu [by TEY (*b*) and CEY (*c*)], respectively. The oxide film thicknesses were 19 nm and 39 nm, respectively.

not consider elastic scattering, the decay length may be short, thus potentially leading to underestimation of the film thickness.

Frazer *et al.* (2003) and Abbate *et al.* (1992) studied the analysis depth in the low-energy region using soft X-rays, and reported that it is not significantly different from the escape depth of Auger electrons without cascade of inelastic scattering. In this study, we investigated Si, an element with a small atomic number, and Cu, an element with a relatively large atomic number. However, our proposed equation may not be applicable at low energies below 1000 eV and in the soft X-ray region. Therefore, this method is limited to elements with atomic numbers above Si.

Table 1
Fractions of Si K-edge and Cu K-edge X-ray absorption near-edge structure spectral components for oxidized Si and oxidized Cu, respectively, which were obtained by fitting the spectrum to a linear combination of standard spectra; the derived factor k is also provided.

| Sample (film thickness) | Measurement mode | Fraction | | Derived factor k |
		Film	Substrate	
Oxidized Si (19 nm)	TEY	39%	61%	6.5
Oxidized Cu (39 nm)	TEY	42%	58%	6.7
	CEY	43%	57%	6.7

Table 2
Thickness derived by the film thickness determination method proposed in this study for the Cu film reported by Girardeau et al. (1992).

Film thickness (nm)†	Film fraction†	Derived thickness (nm)	Error
5	8%	4	−21%
10	15%	8	−23%
20	28%	16	−22%
40	52%	35	−13%
80	82%	82	2%
160	97%	167	4%

† The values were taken from Girardeau et al. (1992).
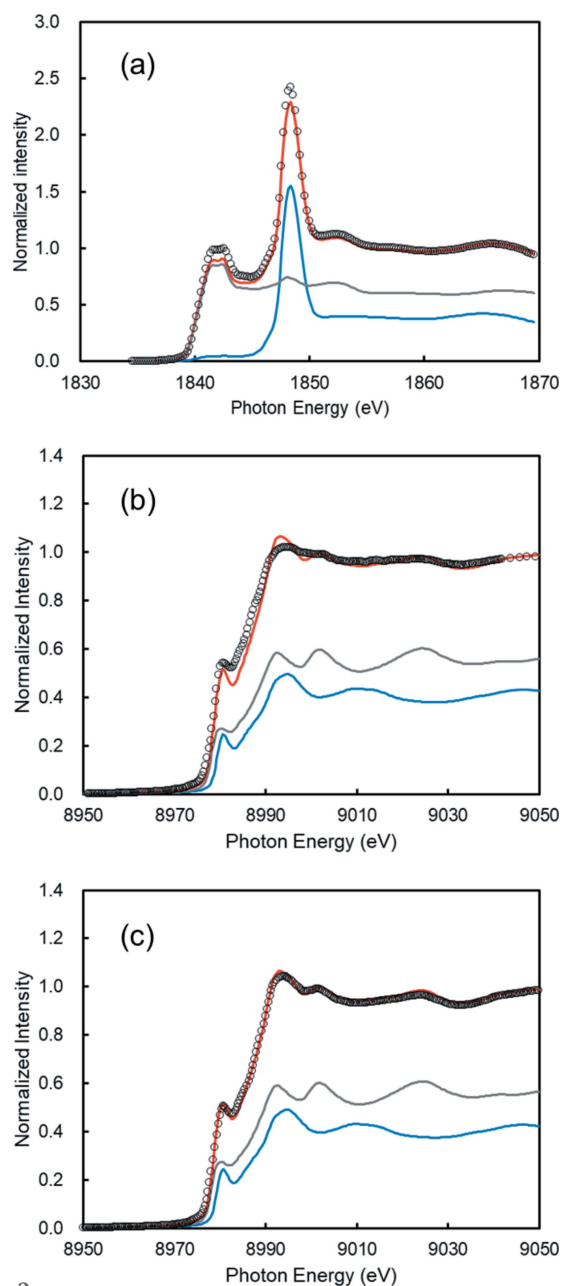
Figure 2
Linear combination fitting results of X-ray absorption near-edge structure spectra for oxidized Si (a) and oxidized Cu [by TEY (b) and CEY (c)]. Gray and blue lines indicate the substrate (Si, Cu) and film (SiO₂, Cu₂O), respectively, while circles and red lines indicate the data and fit, respectively.

5. Conclusions

In this study, we proposed a practical method for deriving film thickness in TEY-XAS. The equation used was modified from the logarithmic equation used in the field of electron spectroscopy, and the modification factor (multiple of the decay length) was experimentally determined using oxidized Si and Cu with films of thickness 19 nm and 39 nm, respectively. The proposed method was validated using the literature, which demonstrated the variation of the film component intensity with the sample film thickness. Although the proposed method requires synchrotron radiation, it can easily determine the film thickness in the range of the TEY-XAS (as well as CEY-XAS) analysis depth (e.g. up to 160 nm for Cu) and can be used in the analysis of various materials with thin films.

Acknowledgements

References

Abbate, M., Goedkoop, J. B., de Groot, F. M. F., Grioni, M., Fuggle, J. C., Hofmann, S., Petersen, H. & Sacchi, M. (1992). *Surf. Interface Anal.* **18**, 65–69.

Bouldin, C. E., Forman, R. A. & Bell, M. I. (1987). *Phys. Rev. B*, **35**, 1429–1432.

Cheng, X.-B., Zhang, R., Zhao, C.-Z., Wei, F., Zhang, J.-G. & Zhang, Q. (2016). *Adv. Sci.* **3**, 1500213.

De Los Santos Valladares, L., Salinas, D. H., Dominguez, A. B., Najarro, D. A., Khondaker, S. I., Mitrelias, T., Barnes, C. H. W., Aguiar, J. A. & Majima, Y. (2012). *Thin Solid Films*, **520**, 6368–6374.

Elam, W. T., Kirkland, J. P., Neiser, R. A. & Wolf, P. D. (1988). *Phys. Rev. B*, **38**, 26–30.

Erbil, A., Cargill, G. S. III, Frahm, R. & Boehme, R. F. (1988). *Phys. Rev. B*, **37**, 2450–2464.

Frazer, B. H., Gilbert, B., Sonderegger, B. R. & De Stasio, G. (2003). *Surf. Sci.* **537**, 161–167.

Girardeau, T., Mimault, J., Jaouen, M., Chartier, P. & Tourillon, G. (1992). *Phys. Rev. B*, **46**, 7144–7152.

Hata, S., Kai, Y., Yamanaka, I., Oosaki, H., Hirota, K. & Yamazaki, S. (2000). *JSAE Rev.* **21**, 97–102.

Hirai, Y., Yasuami, S., Kobayashi, A., Hirai, Y., Nishino, J., Shibata, M., Yamaguchi, K., Liu, K.-Y., Kawado, S., Yamamoto, T., Noguchi,

S., Takahashi, M., Konomi, I., Kimura, S., Hasegawa, M., Awaji, N., Komiya, S., Hirose, T., Ozaki, S., Okajima, T., Ishikawa, T. & Kitamura, H. (2004). *Nucl. Instrum. Methods Phys. Res. A*, **521**, 538–548.

Ishida, A. & Sato, M. (2003). *Acta Mater.* **51**, 5571–5578.

Isomura, N., Cui, Y.-T., Murai, T., Oji, H. & Kimoto, Y. (2017). *J. Appl. Phys.* **122**, 025307.

Kaiser, N. (2002). *Appl. Opt.* **41**, 3053.

Kasrai, K., Lennard, W. N., Brunner, R. W., Bancroft, G. M., Bardwell, J. A. & Tan, K. H. (1996). *Appl. Surf. Sci.* **99**, 303–312.

Kawaura, H., Harada, M., Kondo, Y., Kondo, H., Suganuma, Y., Takahashi, N., Sugiyama, J., Seno, Y. & Yamada, N. L. (2016). *Appl. Mater. Interfaces*, **8**, 9540–9544.

Klysubun, W., Kidkhunthod, P., Tarawarakarn, P., Sombunchoo, P., Kongmark, C., Limpijumnong, S., Rujirawat, S., Yimnirun, R., Tumcharern, G. & Faungnawakij, K. (2017). *J. Synchrotron Rad.* **24**, 707–716.

Nonaka, T., Okuda, C., Kondo, Y., Seno, Y. & Ukyo, Y. (2007). *AIP Conf. Proc.* **882**, 678–680.

Norman, D. (1986). *J. Phys. C: Solid State Phys.* **19**, 3273–3311.

Owens, A., Fraser, G. W. & Gurman, S. J. (2002). *Radiat. Phys. Chem.* **65**, 109–121.

Powell, C. J. & Tanuma, S. (2016). *Hard X-ray Photoelectron Spectroscopy (HAXPES)*, Vol. 59 of *Springer Series in Surface Sciences*, edited by J. Woicik, pp. 111–140. Springer.

Ravel, B. & Newville, M. (2005). *J. Synchrotron Rad.* **12**, 537–541.

Ruosi, A., Raisch, C., Verna, A., Werner, R., Davidson, B. A., Fujii, J., Kleiner, R. & Koelle, D. (2014). *Phys. Rev. B*, **90**, 125120.

Schroeder, S. L. M. (1997). *J. Phys. IV France*, **7**, C2-153–C2-154.

Schroeder, S. L. M., Moggridge, G. D., Ormerod, R. M., Rayment, T. & Lambert, R. M. (1995). *Surf. Sci.* **324**, L371–L377.

Strohmeier, B. R. (1990). *Surf. Interface Anal.* **15**, 51–56.

Takahashi, M., Harada, M., Watanabe, I., Uruga, T., Tanida, H., Yoneda, Y., Emura, S., Tanaka, T., Kimura, H., Kubozono, Y. & Kikkawa, S. (1999). *J. Synchrotron Rad.* **6**, 222–224.

Tanuma, S., Powell, C. J. & Penn, D. R. (1994). *Surf. Interface Anal.* **21**, 165–176.

Tougaard, S. (2000). *QUASES-IMFP-TPP2M* Ver. 3.0, http://www.quases.com/products/quases-imfp-tpp2m/.

Truijen, I., Van Bael, M. K., Rul, H. V. D., D'Haen, J. & Mullens, J. (2007). *J. Sol-Gel Sci. Technol.* **41**, 43–48.

Yamamoto, M., Yoshida, T., Yamamoto, N., Yoshida, H. & Yagi, S. (2014). *e-J. Surf. Sci. Nanotechnol.* **12**, 299–303.

Yoshikawa, H. & Shimizu, R. (1992). *J. Vac. Sci. Technol. A*, **10**, 2931–2937.